Australian Journal of Basic and Applied Sciences, 5(5): 135-146, 2011
ISSN 1991-8178

Computation of Cable Ampacity by Finite Element Method Under Voluntary Conditions

[1]Amin Mahmoudi, [2]Solmaz Kahourzade, [3]R.K.Lalwani

[1]Engineering Department, Help College of Art and Technology, Klang, 41050 Selangor, Malaysia.
[2]Electrical Engineering Department, University of Malaya, 50603 Kuala Lumpur, Malaysia.
[3]Mechanical Engineering Department, University of Malaya, 50603 Kuala Lumpur, Malaysia.

Abstract: This paper presents a new approach for the determination of underground cable ampacity that considers natural convection of air inside a conduit and heterogeneous soil around the conduit, and compares calculated results with conduit-less considerations. It shows how ampacity of a buried cable is affected by thickness of the soil above it, and by the surrounding soil's heterogeneity and thermo-physical characteristic. Commercial ANSYS software for three-dimensional simulation of a $400kV$ polyethylene-paper cables with copper segments is used. The investigation yields numerical solutions for Fourier conducting heat transfer, continuity, energy, and momentum equations. Poor convection of air in conduit is shown to result in cable threshold temperature to be greater than that in conduit-less, other conditions being similar. Also results show that the longer the conduit, the lesser the acceptable ampacity. The proposed method gives criterion and flexibility to change strategy for situations which are not discussed in standard literature on cable routing.

Key words: Underground Cables, Ampacity, Finite Element Method, ANSYS.

Nomenclature:

f	system frequency [Hz]
U	cable operating voltage (phase to phase) [V]
C	electrical capacitance [F]
θ	conductor temperature [$°C$]
θ_{amb}	ambient temperature [$°C$]
H	burial depth under the earth surface [m]
I	current [A]
T	operating temperature [$°C$]
ρ	thermal resistivity [$°K.m/w$]
S	cross-sectional area of conductor [mm^2]
W_c	losses in conductor per unit length [w/m]
W_d	dielectric losses per unit length per phase [w/m]
W_I	total Ohmic power loss of each cable [w/m]
W_t	total power dissipated in cable per-unit [w/m]
ε	relative permittivity of insulation
$tan\ \delta$	loss factor of insulation
y_s	skin effect factor
y_p	proximity effect factor
D_i	external diameter of insulation [m]
dc	external diameter of conductor [m]
λ_1	ratio of the total losses in metallic sheath
λ_2	ratio of the total losses in metallic armor

Corresponding Author: Amin Mahmoudi,Engineering Department, Help College of Art and Technology, Klang, 41050 Selangor, Malaysia.
Tel: +60136778050; Fax: 03-7967 5317;
Email: amaminmahmoudi@gmail.com

α_{20} temperature coefficient at 20 degrees of Celsius
ρ_{20} resistance at 20 degrees of Celsius
R' dc conductor resistance $[\Omega/m]$
R ac conductor resistance $[\Omega/m]$
U_0 phase to ground voltage $[V]$
G_r Grashoff Number
L conduit lenght $[m]$
D conduit diameter $[m]$

INTRODUCTION

Ampacity (current-carrying capacity) determination of an underground cable system is important from theoretical and practical consideration, owing to the risk of temperature rise and the material failure. This work introduces heat transfer mechanism in underground cable installation and analyzes available diffusion equations by using finite element method for natural convection of air inside the conduit and heterogeneous soil around the conduit. The heat transfer mechanism investigated in the present research includes numerical solutions for Fourier conducting heat transfer, continuity, energy, and momentum equations (Holman, 2002; Lewis, 2004). From the present literature survey to the best of the authors' knowledge no work has been publish for the heterogeneous soil. However, in the 1950s Neher and McGrath (1957) proposed a model that was accepted for calculation of underground-cable ampacity only for homogenous soil. The thermal model is based on a number of simplifying assumptions, making mathematical formulation easier; and one of the assumptions is that there are neither thermal nor geometrical changes along the entire cable route. The assumption decreases to two dimensions from a three-dimensional formulation. Further, the two-dimensional analysis is decreased, via principle of superposition, to a one-dimensional heat transfer problem that makes use of a virtual heat sink of the same values above earth's surface at a distance equal to the buried depth. Finding the cable ampacity is thus reduced to direct solving of an algebraic equation (1957). The mathematical approximation provides values for an ampacity table. The values are accepted as being the standard ampacity of most underground cable systems (IEEE, 1994; IEC 1994; IEC, 1995). The table, however, does not provide instructions for determination of ampacity when thermal changes occur along cable length (Hwang, 2000) as happens for instance, when a cable crosses a paved parking lot, so conductor temperature increases (Brakelmann, 2001). In more complex situations, thermal conditions exist for a long sector of the route, that it is better to base design of the entire cable system on a combination of the worst thermal conditions (Nahman, 2002). F. Aras *et al.* (2005) present an assessment of methods that calculate ampacity of underground power cables. All the above mentioned research works are limited to homogenous soils. In addition, they ignored the natural convection inside the conduit owing to variable thermal resistance of the air layer which is the quantity that varies with the temperature.

When there are poor thermal conditions in only a short proportion of the entire cable route, there is no clear guide to the amount of cable ampacity derating (Hwang, 2000; Brakelmann, 2001; Nahman, 2002; Aras, 2005). The situation unfortunately often happens when the cable must pass through a relatively short segment of conduit or when the cable shares underground space with other utilities. Power cables are usually installed in urban areas and the thermal conditions along their route are rarely fixed. Even if there is no street crossing, the existence of vegetation significantly changes the local thermal environment. The temperature of a buried cable crossing an area of unfavorable thermal characteristics is higher than that in a uniform environment. A deviation from the cable ampacity values presented in ampacity standards is however inevitable along the cable route and variations limit heat transfer to earth's surface. New approaches to assessment of underground cable performance are thus presented (Vaucheret, 2005; Al-Saud, 2008; Leon, 2008). Finite Element Analysis (FEA) of underground cables has been studied by many researchers for homogenous soil without natural air convection inside the conduit (Hwang, 2000; Al-Saud, 2008). This paper presents Finite Element Method (FEM) and considers natural air convection inside conduit and heterogeneous soil around cable conduit which has not been reported earlier. FEM is more powerful and more precise in complex geometrical modeling.

Summarizing, cable ampacity is greatly affected by cable installation conditions and the properties of the material surrounding the cable. Factors affecting ampacity studied here are soil thermal resistivity, cable burial depth, directly-buried versus duct-bank-installed, and length of conduit. The work aims to determine, via three-dimensional analysis, how current decreases when an underground cable is routed through a short section of conduit in heterogeneous soil.

Current through a cable produces both heat and electromagnetic field that affect ampacity of other cables near it, so neighboring effects are also considered in the simulations on the ANSYS software.

2. *Modeling:*

The following specifications are for the cable in the present analysis: 400 *kV* polyethylene-paper cable with copper segments, 85°*C* maximum operating temperature (*T*), 60 *Hz* system frequency (*f*), 2.8 relative permittivity (ε) of insulation, and 0.001 insulation loss factor ($tan\ \delta$); as shown in Fig. 1 (Anders, 2005) for results comparison with homogenous soil condition.

Calculation of ampacity for a cable routed through various environments is complicated. The existence of the conduit, heterogeneous soil and natural convection create a three-dimensional heat transfer problem. Temperature distribution is a function of axial location, radial distance from cable, variable soil resistance and depth beneath the earth's surface. To compare our results with the standard tables (IEEE, 1994; IEC, 1995) firstly, an example of cable installation as shown in Fig. 2 is simulated. The results are then compared for homogeneous soil without conduit only; because for heterogeneous soil and natural convection consideration no standards are available. This is done just to ensure the validity of our method for heterogeneous and natural convection cable system. The cable parameters are provided in table 1. It includes the general data of the cable and calculated data for three-phase cable system in standard installation as indicated in Fig. 2.

2.1. *Assumptions:*

- For simple modeling of the problem, the following assumptions were made:
- Steady-state conditions
- Soil and conduit properties are constant and independent of temperature.
- Open-circuited cable shielded
- Conduit's thickness is thin and its thermal resistance is the same as the surrounding soil; so thermal resistance of conduit rim adds to resistance of adjacent soil layer.
- The only quantity varying with temperature is thermal resistance of the air layer.
- The vertical plane perpendicular to the cable axis at the center of the conduit and the vertical plane through the cable centerline are adiabatic planes.
- Regions of the soil far from the cable are maintained at ambient soil temperature.
- Ambient soil temperature is 25 degrees Celsius.
- Temperature-dependent thermal resistance of air layer in conduit, and free convection.
- Soil condition may be homogeneous or heterogeneous.

The last two assumptions have not been considered by earlier authors. These assumptions make the results more versatile and applicable to very general actual conditions.

2.2. *Finite Element Method:*

To determine cable ampacity, finite element software package ANSYS 10 (ANSYS) and (GAMBIT) for auto mesh generation are used. Solving heat transfer problems typically consists of calculating field temperature for given heat input rates. To calculate ampacity of a cable system by using finite element software with thermal capabilities, the inverse problem must be solved. Heat input rate is used to determine for threshold temperature of the cable conductor. The target temperature is 85 degrees Celsius. For a range of electrical current, temperature distribution in the entire domain is thus computed iteratively until maximum cable temperature reaches threshold value.

The proposed approach requires building a finite element mesh and solving the resulting heat transfer equations for the temperature at the cable surface. Fig. 3 shows three-dimensional mesh by using tetrahedral elements with 6 nodes to fit the circular shapes of 8 layers starting from the core to the surrounding soil by GAMBIT software. GAMBIT is used only to auto generate the finite element mesh and simulation is analyzed on ANSYS software. GAMBIT software generated 120956 elements in various iterations. After having the mesh with optimum number of elements which is 120956 then to assure no further increase in the number of elements will affect the results; the numbers of elements are doubled and the simulations confirmed as having the same results as in the other case. Finite element analysis relies on type of elements, whose choice affect results significantly. In the simulations, TGrid-Map element, which is tetrahedral and well-suited to round shapes such as cable cross section, is chosen.

Soil conductivity is more important because it plays very important role while the resistance of air on earth's surface has no significant influence so it is neglected, and soil surface considered as isothermal.

The energy produced, owing to the cable's electric current, is considered as a heat source, and infinite boundary conditions are applied to all the other surfaces. Also, in conduit-installed cable, considering acceleration due to gravity to be 9.81 m/s^2 and by Boussinesq approximation, the air around the cables gives Grashoff number G_r less than 10^{10}, meaning airflow inside the conduit is laminar (Mahmoudi, 2008).

2.3. *Applying the Current:*

Maximum temperature of a high-voltage cable is determined by threshold temperature of the cable's insulation. The temperature is due to energy generated through Ohmic and dielectric losses, which, in the simulation, are considered heat sources. To calculate the heat generated by the current in cable; its resistance must be known. Conductor resistance is calculated in two stages. The dc conductor resistance $R'(\Omega/m)$ is first obtained from the following equation:

$$R' = \frac{1.02\times10^{6}\rho_{20}}{S}[1+\alpha_{20}(\theta-20)] \tag{1}$$

where,
ρ_{20} is conductor resistance at 20 degrees of Celsius,
α_{20} is temperature coefficient at 20 degrees of Celsius,
θ is conductor temperature [$°C$],
S is cross-sectional area of conductor [mm^2].

R' is then modified to take into account skin and proximity effects. The resistance of a conductor when carrying alternating current is higher than that when carrying direct current. The principal reasons for the increase are skin effect, proximity effect, hysteresis and eddy current
losses in nearby ferromagnetic materials, and induced losses in short-circuited non-ferromagnetic materials. For conductor losses, only skin and proximity effects, and in some cases approximation of metallic sheath effect, are considered, except in very high voltage cables consisting of large segmental conductors. The relevant expressions are:

$$R = R'(1+y_s+y_p) \tag{2}$$

$$W_c = R\cdot I^2 \tag{3}$$

where, $R(\Omega/m)$ and $W_c(w/m)$ are the conductor's ac resistance and losses, respectively. y_s and y_p are skin effect and proximity effect, respectively. Sheath losses are current and bonding dependent, and can be divided into two categories. The losses are due to current circulating in single-core-cable and divided in to eddy current circulating radially (skin effect) and azimuthally (proximity effect). Eddy current losses occur in both three-core and single-core cables, regardless of bonding. Eddy current losses in solidly bonded single-core-cable sheaths are negligible. So, they are ignored except for cables with large segmental conductors. Cable losses W_I can thus be expressed as:

$$W_I = W_c + W_s + W_a = W_c(1+\lambda_1+\lambda_2) \tag{4}$$

λ_1 is called sheath loss factor, and is equal to the ratio of total losses in the metallic sheath to total losses. λ_2 is armor loss factor, and is equal to the ratio of total losses in the metallic armor to total losses of conductor. When paper and solid dielectric insulations are subjected to alternating voltage, they act as large capacitors. Each time voltage direction changes, realignment of electrons (i.e., 50 or 60 times a second) produce heat. It results in loss of real power called dielectric loss. For a unit length of cable, magnitude of the required charging current is a function of dielectric insulation constant, dimensions of the cable, and operating voltage. For some cable arrangements (notably for high-voltage, paper insulated) this loss can significantly affect cable rating. Dielectric losses are computed from the following expression:

$$W_d = 2\pi\cdot f\cdot C\cdot U_0^2\cdot\tan\delta \tag{5}$$

where, the electrical capacitance C and the phase to ground voltage U_0 are obtained from:

$$C = \frac{\varepsilon}{18\ln\left(\frac{D_i}{d_c}\right)}\cdot10^{-9} \tag{6}$$

$$U_0 = \frac{U}{\sqrt{3}} \tag{7}$$

It is convenient to express all heat flows due to power losses in the cable in term of the loss per meter of the conductor. From equations (4) and (5) the total loss *Wt* is computed from:

$$W_t = W_I + W_d = W_c(1 + \lambda_1 + \lambda_2) + W_d \tag{8}$$

3. *Simulation Results, Verification and Discussion:*

3.1. *Simulation Verification:*

To validate present results, simulations are done using ANSYS software for standard homogenous soil conditions for a three-phase cable system buried underground in soil with thermal resistivity of 1°*K.m/w* and 1.8*m* depth. Table 2 shows the calculated cable's ampacity is 1363*A*, which is then confirmed against the standards. The cable's current capability when buried through a conduit considering the free laminar convection and homogenous soil with thermal resistivity of 1°*K.m/w* shows a 20% decrease, from 1363*A* to 1098*A*. Both conduit-less and through-conduit installations of a single-phase cable system buried in similar conditions are simulated. The results are very close to the ones presented in the standard that shows the validity of present simulation approach. Fig. 4 compares cable-ampacity standard values, presenting ampere values against various soils' resistivity. Results of the simulation show conformance to standard data.

Figs. 5 and 6 show the temperature contours of the cables, one cable conduit-less, the other with conduit. The contours are found to be symmetrical in the x-y planes. As expected, temperature varies significantly upwards earth's surface than away from it as shown in Figs. 5(a) and 6(a). Thermal dissipation for with-conduit is generally similar to that for conduit-less except for poor air convection inside conduit delaying convergence to ambient temperature at earth's surface.

Figs.7 (a) and 7(b) show air moving inside the conduit, owing to natural convection in y-z plane (in front). There is no evident air flow at the bottom of the conduit, owing to gravity-caused obstruction at the contact between cable and conduit. Motion vectors of the air inside the conduit are symmetrical for single-phase, but unsymmetrical for two-sided cables in three-phase. In both, high velocity is seen to occur at cable surface and at conduit rim. The phenomenon can be explained by the interaction of heat generation, gravity, and geometry effect (such as conduit size). Figs. 8 (a) and 8 (b) demonstrate temperature contour and air-motion vector, respectively, in y-z plane. Fig. 8 (a) shows temperature dissipation along wire direction, for three-phase. Its front view is shown in Fig. 6 (a). Fig. 8 (b) is the side view of Fig. 7 (b).

3.2. *Cable Ampacity Buried in Heterogeneous Soil:*

When the soil is heterogeneous, there is no distinct method for determination of cable ampacity. Heterogeneous situation occurs when cable crosses near underground facilities or trees. Each variation restricting thermal conduction toward ground surface de-rates cable ampacity compared to the ones presented in standard tables (IEEE, 1994; IEC, 1995).

To investigate the effect of heterogeneous soil, the soil is divided into 27 sections by computer generation random numbers for soil sections thermal resistivity. Fig. 9 shows each heterogeneous soil segment's thermal resistivity in terms of °*K.m/w*. In this case, cables are installed in standard position as section 2. Simulations consider the same boundary conditions and load application. Temperature contours achieved are non-monotonous, varying in different directions.

Fig.10 (a) and (b) show front and side views of the temperature contours for three-phase conduit in heterogeneous soil. Temperature distribution is not symmetrical in any direction. Heat transfer seems to be towards the less-thermal-resistance region. The random selection of soil resistivity made heat distribution random. Table 3 compares values achieved for the heterogeneous soil and the homogenous soil.

3.3. *Factors Affecting Cable Ampacity:*

Effect of Soil Resistivity:

Fig. 11 shows cable ampacity varying with change of soil resistivity, for both the with-conduit and the conduit-less cables. Cable ampacity is proportional to soil conductivity; rising soil conductivity dissipates more heat, increasing cable ampacity.

Effect of Cable Depth:

Fig. 12 shows how burial depth affects the ampacity of cables buried with conduit and conduit-less, in both homogeneous soil and heterogeneous soil. Increases in soil depth are seen to reduce conductivity; less

heat dissipation, less ampacity. Rate of cable ampacity changes is higher the nearer the cable is to earth's surface.

Effect of Conduit Length:

Determining the effect of conduit length on cable ampacity of the buried cables is a significant application of the finite element software. To find the effect of conduit length on ampacity, simulation is carried out for different length. Fig. 13 shows the trend for cable ampacity of a three-phase cable buried in a conduit with different length. Cable ampacity is plotted against dimensionless specific lengths quantified by the ratio of conduit length (L) to conduit diameter (D). Fig. 13 shows a decline in ampacity of the cable as expected as conduit lengthened. The result indicates full de-rating of the cable upon lengthening of the conduit to approximately 10 times the conduit's diameter. The cable thus no longer needs further de-rating, and its ampacity to be estimated according to existence of the entire cable route inside conduit.

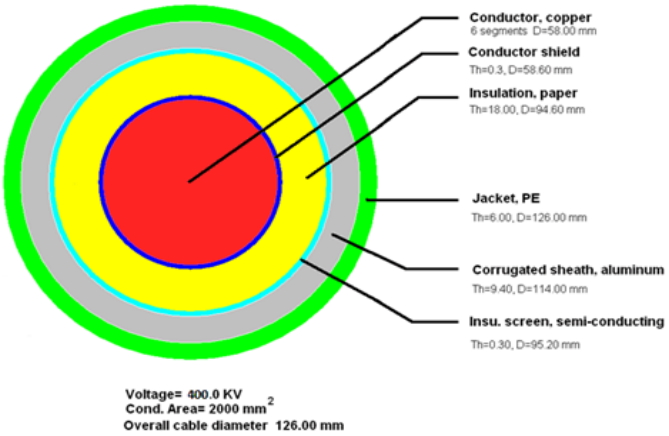

Fig. 1: Cross-section of cable (Anders, 2005).

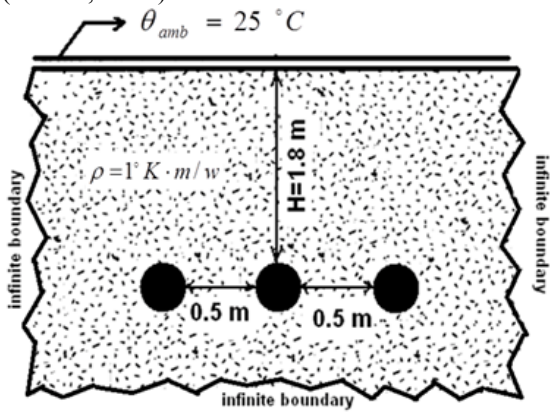

Fig. 2: Standard cable-laying condition.

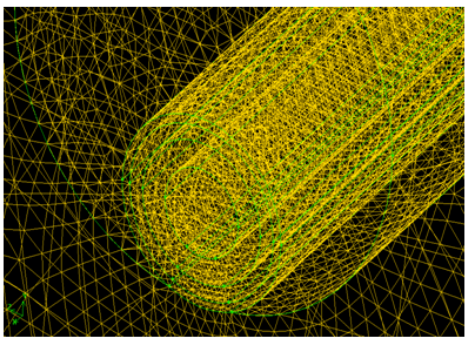

Fig. 3: Auto mesh generation by GAMBIT software (GAMBIT).

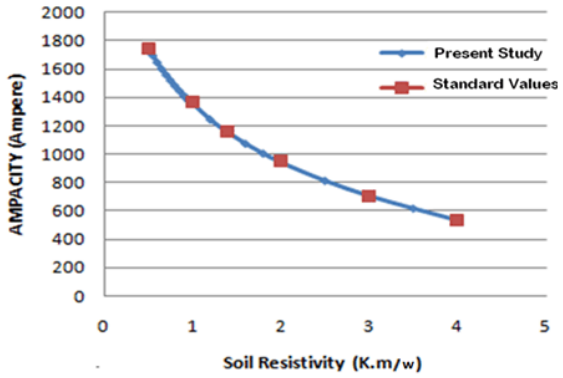

Fig. 4: Comparison of present study with the standard values for homogenous conduit-less underground cable.

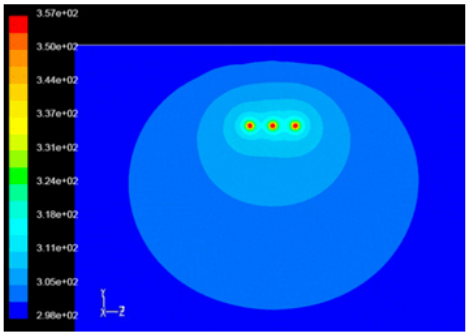

(a) Three-phase

Fig. 5: Temperature (°K) contours of the conduit-less underground cable.

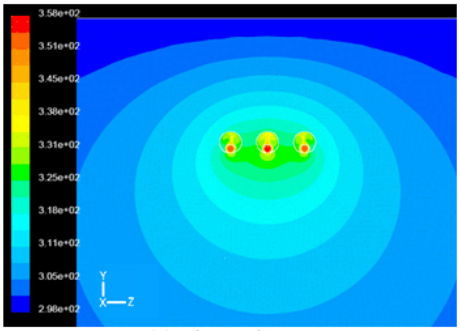

(a) Three-phase

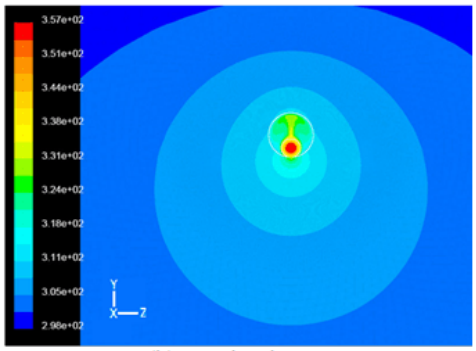

(b) Single-phase

Fig. 6: Temperature (°K) contours of the cable buried with conduit.

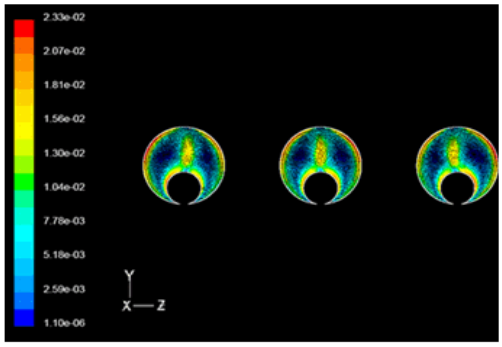

(a) Three-phase

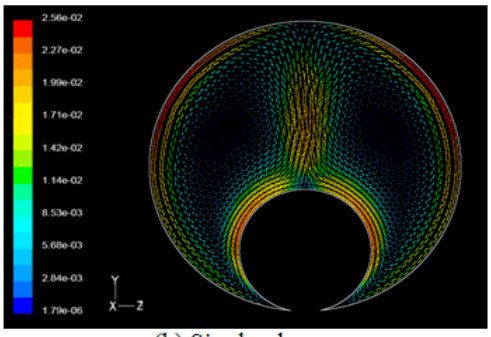

(b) Single-phase

Fig. 7: Motion vectors (m/s) of the air inside the conduit due to natural convection.

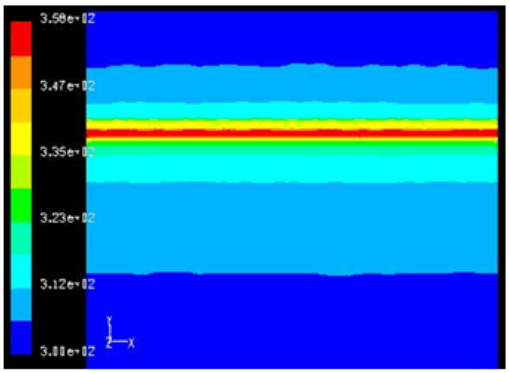

(a) Temperature Contour

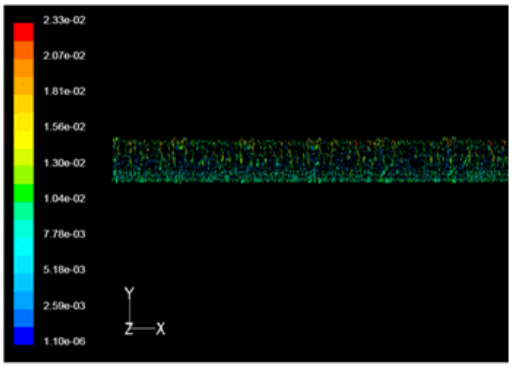

(b) Motion vector

Fig. 8: Temperature (°K) contours and motion vectors (m/s), from X-Y plane direction.

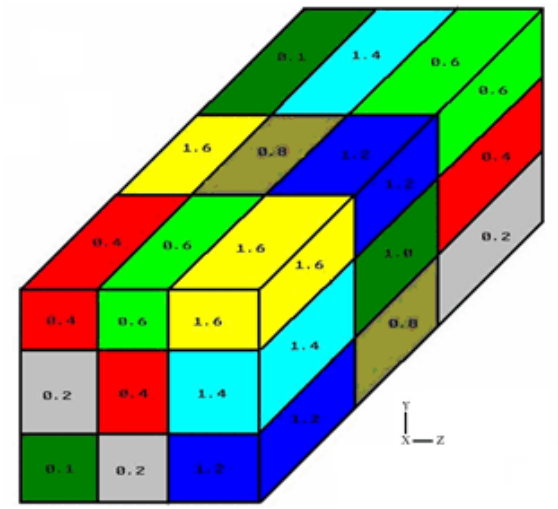

Fig. 9: Computer generated random heterogeneous soil segments.

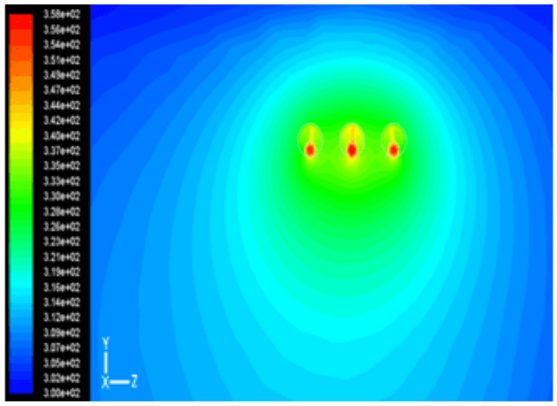

(a) front view of temperature counter

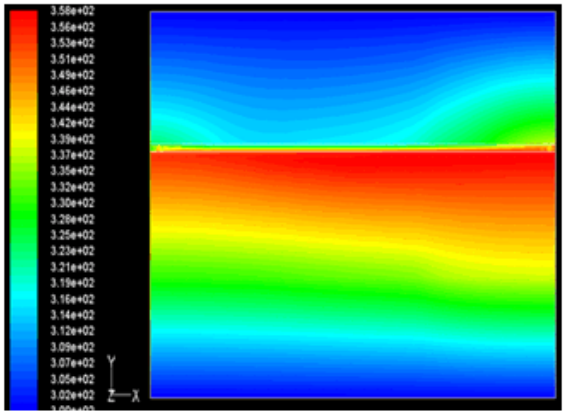

(b) side view of temperature counter

Fig. 10: Two views of the temperature (°K) contours of the cable buried with conduit in heterogeneous soil.

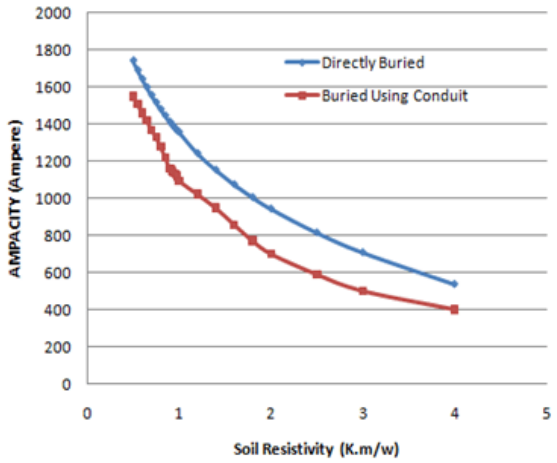

Fig. 11: Change of cable ampacity with respect to soil resistivity.

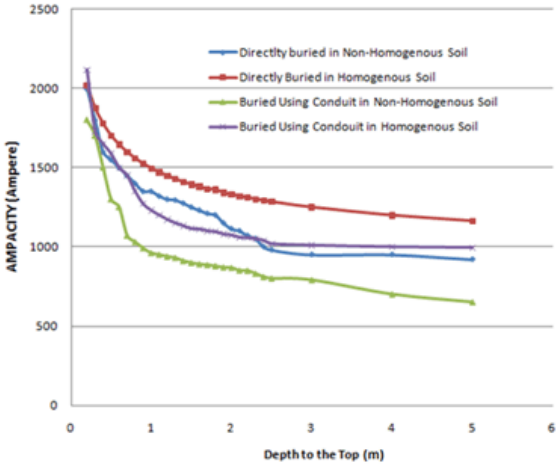

Fig. 12: Change of cable ampacity with respect to burial depths.

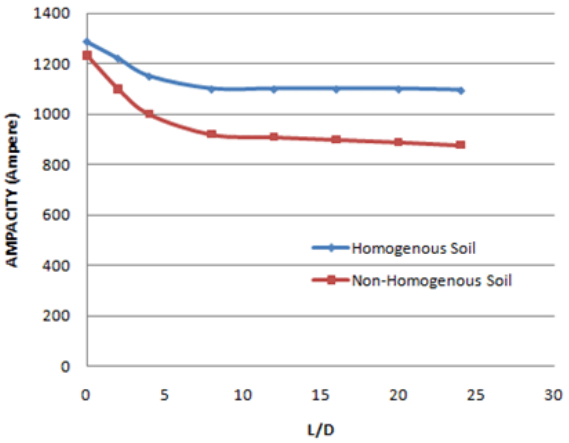

Fig. 13: Change of cable ampacity with respect to (L/D) non-dimensional conduit length.

Table 1: Parameters of the simulated cable.

	General Data		
θ	85 C	ε	2.8
f	60 (Hz)	tan δ	0.001
	Calculated data for 3-phase cable system in standard installation		
ys	0.132	y_p	0.005
λ_1	0.150	λ_2	0
R	0.0126 (Ω/km)	W_c	23.40 (w/m)
W_I	26.92(w/m)	W_d	6.53 (w/m)
I	1365 (Amp)	W_T	33.45 (w/m)

Table 2: Simulation and standard values.

	ANSYS Simulation	Standard	Deviation from standard
Three-phase, conduit-less	1363	1365	0.00146734
Three-phase, inside coduit	1098	1100	0.00182493
Single-phase, conduit-less	1739	1735	-0.00230017
Single-phase, inside conduit	1347	1350	0.00227171

Table 3: Heterogeneous and homogenous soil ampacity.

	Heterogeneous [Simulation]	Homogenous [Simulation]	Heterogeneous [Standard]
Three-phase, conduit-less	1232	1363	1365
Three-phase, inside coduit	878	1100	1100
Three-phase, conduit-less	1556	1739	1735
Single-phase, inside conduit	1172	1350	1350

Conclusions:

The proposed approach determines fairly well the maximum load current allowable on underground cables in voluntary conditions. Its analyses can be applied to assessing cable ampacity in various environments and installation conditions, even heterogeneous soil. Results show that cable ampacity depends on cable geometry and installation, burial depth, and thermal resistivity of soil. Cable ampacity is proportionate to soil conductivity; when soil conductivity rises, cable ampacity increases as more heat is dissipated. Results show cable ampacity decreases with increased depth of cable installation under the soil surface. Simulations show poor free convection of air in conduit resulting cable threshold temperature to be greater than that in conduit-less, other conditions remaining the same. Also, as conduit length increases, acceptable ampacity reduces. Once conduit length reaches 10 times its diameter length, further de-rating of cable ampacity becomes unnecessary. This approach gives a suitable criterion and a flexible change-strategy for cases like heterogeneous soil and free air laminar convection which can be now incorporated in standard literatures on cable routing.

REFERENCES

Al-Saud, M.S., M.A. El-Kady, R.D. Findlay, 2008. A New Approach to Underground Cable Performance Assessment, Journal of Electric Power Systems Research, 78(5): 907-918.

Anders, G., 2005. Rating of Electric Power Cables in Unfavorable Thermal Environments (IEEE Press. New York.

Aras, F., C. Oysu, G. Yilmaz, 2005. An Assessment of the Methods for Calculating Ampacity of Underground Power Cables, Electric Power Components and Systems, 33 (12): 1385-1402.

ANSYS Finite Element Simulation Software. ANSYS Inc. PA. Canonsburg.

Brakelmann, H., G. Anders, 2001. Ampacity Reduction Factors for Cables Crossing Thermally Unfavorable Regions, IEEE Transaction on Power Delivery, 16(4): 444-448.

GAMBIT Software Tools Version 0.2010.09.01, available: http://www.gambit-project.org

Holman, J.P., 2002. Heat Transfer 9th Edition McGraw Hill, London.

Hwang, C.C., Y.H. Jiang, 2003. Extensions to the Finite Element Method for Thermal Analysis of Underground Cable Systems, Journal of Electric Power Systems Research, 64(2): 159-164.

Hwang, C.C., J.J. Chang, H.Y. Chen, 2000. Calculation of Ampacities for Cables in Trays Using Finite Elements, Journal of Electric Power Systems Research, 54(2): 75-81.

IEEE Standard Power Cable Ampacity Tables, 1994. IEEE N.Y. Std., 835.

IEC Standard Electric Cables-Calculation of Current Rating-Part 1: Current Rating equations (100% load Factor) and calculation of Losses- Section 1: General, 1994. IEC Std., 287.

IEC Standard Electric Cables-Calculation of Current Rating-Part 1: Current Rating equations (100% load Factor) and calculation of Losses- Section 2: 1994. Sheath Eddy Current Loss Factors for Two Circuits in Flat Formation, IEC Std., 287.

IEC Standard Electric Cables-Calculation of Current Rating-Part 2: Thermal resistance-Section 1: Calculation of thermal resistance, 1994. IEC Std. 287.

IEC Standard, 1995. A Method for Calculating Reduction Factors for Groups of Cables in Free Air, Electric Cables- Calculation of the Current Rating-Part 2: Thermal Resistance – Section 2A: Protected from Solar Radiation, IEC Std., 287.

IEC Standard. Electric Cables- Calculation of the Current Rating-Part 3: Sections on Operating Conditions-Section 1: Reference Operating Conditions and Selection of Cable Type, IEC Std. 287-1995.

Leon, F. de, G.J. Anders, 2008. Effects of Backfilling on Cable Ampacity Analyzed with the Finite Element Method, IEEE Transaction on Power Delivery, 23(2): 537-543.

Lewis, W.P., R. Nithiarasu, K.N. Seetharamu, J. Wiley, 2004. Fundamentals of the Finite Element Method for Heat and Fluid Flow Wiley Online Library.

Mahmoudi, A., 2008. Ampacity Derating Factors for Cables in Different Environmental Conditions by FEM, M.S. Dissertation, Dept. Elect. Eng., Amirkabir University of Technology.

Neher, J.H., M.H. McGrath, 1957. The Calculation of the Temperature Rise and Load Capability of Cable Systems, Power Apparatus and Systems, Part III. Transactions of the American Institute of Electrical Engineers, 76(3): 752-764.

Nahman, J., M. Tanaskovic, 2002. Determination of the Current Carrying Capacity of Cables Using the Finite Element Method, Journal of Electric Power Systems Research, 61(2): 109-117.

Patankar, S.V., 1980. Numerical Heat Transfer and Fluid Flow Hemisphere Pub.

Vaucheret, P., R.A. Hartlein, W.Z. Black, 2005. Ampacity Derating Factors for Cables Buried in Short Segments of Conduit, IEEE Transaction on Power Delivery, 20(2): 560-565.